KANAZAWA-11-17, UT-HET 059

Testing the Higgs triplet model with the mass difference at the LHC

Mayumi Aoki [1], Shinya Kanemura [2], Kei Yagyu [2]
[1] *Institute for Theoretical Physics, Kanazawa University, Kanazawa 920-1192, Japan*
[2] *Department of Physics, University of Toyama, 3190 Gofuku, Toyama 930-8555, Japan*

In general, there can be mass differences among scalar bosons of the Higgs triplet field with the hypercharge of $Y = 1$. In the Higgs triplet model, when the vacuum expectation value v_Δ of the triplet field is much smaller than that v ($\simeq 246$ GeV) of the Higgs doublet field as required by the electroweak precision data, a characteristic mass spectrum $m^2_{H^{++}} - m^2_{H^+} \simeq m^2_{H^+} - m^2_{\phi^0} (\equiv \xi)$ appears, where $m_{H^{++}}$, m_{H^+}, m_{ϕ^0} are the masses of the doubly-charged (H^{++}), the singly-charged (H^+) and the neutral ($\phi^0 = H^0$ or A^0) scalar bosons, respectively. It should be emphasized that phenomenology with $\xi \neq 0$ is drastically different from that in the case with $\xi = 0$ where the doubly-charged scalar boson decays into the same sign dilepton $\ell^+\ell^+$ or the diboson W^+W^+ depending on the size of v_Δ. We find that, in the case of $\xi > 0$, where H^{++} is the heaviest, H^{++} can be identified via the cascade decays such as $H^{++} \to H^+ W^{+(*)} \to \phi^0 W^{+(*)} W^{+(*)} \to b\bar{b}\ell^+\nu\ell^+\nu$. We outline how the Higgs triplet model can be explored in such a case at the LHC. By the determination of the mass spectrum, the model can be tested and further can be distinguished from the other models with doubly-charged scalar bosons.

PACS numbers: 12.60.-i, 12.60.Fr, 14.80.Ec, 14.80.Fd

I. INTRODUCTION

In spite of its crucial role to trigger the electroweak symmetry breaking, the Higgs sector remains unknown, and its essence is still mysterious. Exploration of the Higgs sector is the most important issue in current high energy physics. Recent results of Higgs boson searches at the Tevatron and the LHC have strongly constrained the mass of the Higgs boson in the Standard Model (SM) to be from 114 GeV to 145 GeV [1]. The Higgs boson is expected to be discovered in near future at the LHC as long as the SM-like picture effectively holds.

At the same time there is no strong motivation to the minimal form of the Higgs sector proposed in the SM, where only one scalar doublet field is introduced. In fact, extended Higgs sectors are often considered in the context of various scenarios for physics beyond the SM, in which new phenomena such as neutrino oscillation [2], dark matter [3] and/or baryon asymmetry of the Universe [4] are explained.

In order to explain tiny masses of neutrinos, several scenarios have been proposed in the literature, in which a source of lepton number violation is introduced with additional Majorana neutrinos [5], a triplet scalar field [6] or triplet fermion fields [7]. In particular, the second possibility; i.e., the Higgs Triplet Model (HTM), where a scalar triplet field with the hypercharge $Y = 1$[1] is added to the SM, is the simplest model which deduces the extended Higgs sector. Assuming that the triplet scalar field carries two units of lepton number, the lepton number conservation is violated in a trilinear interaction among the Higgs doublet field and the Higgs triplet field. Majorana masses for neutrinos are then generated through the Yukawa interaction of the lepton doublet and the triplet scalar field. When the masses of the component fields of the triplet are at the TeV scale or less, the model can be tested by directly detecting them, such as the doubly-charged ($H^{\pm\pm}$), singly-charged ($H^\pm$) and the neutral scalar bosons.

In addition to the appearance of these charged scalar bosons, a striking prediction of the HTM is the relationship among the masses of the component fields of the triplet scalar field; $m^2_{H^{++}} - m^2_{H^+} \simeq m^2_{H^+} - m^2_{\phi^0} (\equiv \xi)$, where $m_{H^{++}}$, m_{H^+} and m_{ϕ^0} are the masses of $H^{\pm\pm}$, $H^\pm$ and ϕ^0, respectively, where ϕ^0 is H or A with H to be the triplet-like CP-even Higgs boson and A to be the triplet-like CP-odd Higgs boson. The squired mass difference ξ is determined by v ($\simeq 246$ GeV), the vacuum expectation value (VEV) of the doublet scalar field, and a scalar self-coupling constant. As such a mass difference is not forbidden by the symmetry of the model, we may be able to distinguish the model from the others which contain charged Higgs bosons by measuring ξ. Namely, if we discover $H^{\pm\pm}$, $H^\pm$ and ϕ^0 and if we confirm the relationship mentioned above, the model could be identified.

[1] The convention of Y is defined by the relation of $Q = I + Y$.

In the previous studies, the collider phenomenology in the HTM has been discussed mainly by assuming $\xi = 0$ [8–15]. In such a case, H^{++} decays into the same sign dilepton $\ell^+\ell^+$ or the diboson W^+W^+, depending on the size of v_Δ, $m_{H^{++}}$ and also the detail of neutrino masses, where v_Δ is the VEV of the triplet field. These decay modes can be a clear signature for H^{++}. At the same time, H^+ decays into a lepton pair $\ell^+\nu$ or W^+Z [2]. In the case where H^{++} decays into $\ell^+\ell^+$, the pair production process $pp \to H^{++}H^{--} \to \ell^+\ell^+\ell^-\ell^-$ and the associated production process $pp \to H^{++}H^- \to \ell^+\ell^+\ell^-\nu$ would be useful to identify H^{++} and to extract the flavor structure of the model at the LHC [8–15]. The upper bound of $m_{H^{++}}(\gtrsim 250 - 300$ GeV [16]) has been obtained from these processes. In the case where H^{++} decays into W^+W^+, on the other hand, the process $pp \to H^{++}H^{--} \to W^+W^+W^-W^- \to \ell^+\ell^- jjjj\not{E}_T$ and $pp \to H^{++}H^- \to W^+W^+W^-Z \to \ell^+\ell^- jjjj\not{E}_T$ have been studied in Ref. [11].

However, in the case of $\xi \neq 0$, as pointed out in Refs. [10–13, 17], the situation is changed drastically as compared to that of the $\xi = 0$. There are two cases with $\xi \neq 0$ depending on the sign of ξ. If ξ is positive (negative), H^{++} is the heaviest (lightest) of all the triplet-like scalar bosons. In the case of $\xi < 0$, while H^+ can decay into $H^{++}W^{-(*)}$ [12] the decay pattern of H^{++} is the same as in the case of $\xi = 0$. On the other hand, in the case of $\xi > 0$, the cascade decay of H^{++} dominates; i.e., $H^{++} \to H^+W^{+(*)} \to \phi^0 W^{+(*)}W^{+(*)}$ as long as v_Δ is neither too small nor too large[3]. Detailed analyses for collider signature of these processes for $\xi > 0$ have not been studied so far.

In this paper, we focus on the phenomenology of the HTM with the mass difference among the triplt-like scalar bosons at the LHC. In particular, we discuss the case with $\xi > 0$. In this case, the limit of the mass of H^{++} from the recent results at the LHC cannot be applied, so that the triplet-like scalar bosons with the mass of $\mathcal{O}(100)$ GeV are still allowed [4]. We find that $m_{H^{++}}$ may be reconstructed, for example from the process $pp \to H^{++}H^- \to (\phi^0 W^{+(*)}W^{+(*)})(\phi^0 W^{-(*)}) \to (\ell^+\ell^+ b\bar{b}\not{E}_T)(jjb\bar{b})$ by observing the Jacobian peak in the transverse mass distribution of the $\ell^+\ell^+ b\bar{b}\not{E}_T$ system. In addition, m_{H^+} can be reconstructed, for example from the process $pp \to H^+\phi^0 \to (\phi^0 W^{+(*)})(b\bar{b}) \to (\ell^+ b\bar{b}\not{E}_T)(b\bar{b})$ by measuring the Jacobian peak in the transverse mass distribution of the $\ell^+ b\bar{b}\not{E}_T$ system. Furthermore, m_{ϕ^0} can be measured by using the invariant mass distribution of the $b\bar{b}$ system. From these analyses all the masses of the triplet-like scalar bosons may be able to be reconstructed. By measuring these mass differences, we may be able to distinguish models which contain doubly-charged scalar bosons, for instance, doubly-charged scalar bosons from singlet fields which are motivated by the Zee-Babu model [18] and that from doublet scalar bosons which are discussed in Refs. [8, 19, 20].

This paper is organized as follows. In Sec. II, we give a brief review of the HTM. In Sec. III, the decay branching ratios of the triplet-like scalar bosons are evaluated in both the case of $\xi = 0$ and $\xi \neq 0$. In Sec. IV, we outline the mass reconstruction of the triplet-like scalar bosons. Discussions are given in Sec. V, and conclusions are presented in Sec. VI.

II. THE HIGGS TRIPLET MODEL

The Higgs sector is composed of the $Y = 1$ isospin triplet scalar field Δ and the $Y = 1/2$ doublet scalar field Φ. The most general Higgs potential is given by

$$\begin{aligned} V &= m^2\Phi^\dagger\Phi + M^2\mathrm{Tr}(\Delta^\dagger\Delta) + \left[\mu\Phi^T i\tau_2\Delta^\dagger\Phi + \mathrm{h.c.}\right] \\ &\quad + \lambda_1(\Phi^\dagger\Phi)^2 + \lambda_2\left[\mathrm{Tr}(\Delta^\dagger\Delta)\right]^2 + \lambda_3\mathrm{Tr}(\Delta^\dagger\Delta)^2 + \lambda_4(\Phi^\dagger\Phi)\mathrm{Tr}(\Delta^\dagger\Delta) + \lambda_5\Phi^\dagger\Delta\Delta^\dagger\Phi. \end{aligned} \tag{1}$$

The component fields of Φ and Δ can be parameterized as

$$\Phi = \begin{bmatrix} \varphi^+ \\ \frac{1}{\sqrt{2}}(\varphi + v + i\chi) \end{bmatrix}, \quad \Delta = \begin{bmatrix} \frac{\Delta^+}{\sqrt{2}} & \Delta^{++} \\ \Delta^0 & -\frac{\Delta^+}{\sqrt{2}} \end{bmatrix}, \quad \Delta^0 = \frac{1}{\sqrt{2}}(\delta + v_\Delta + i\eta). \tag{2}$$

Imposing the vacuum condition, we can eliminate m^2 and M^2 as

$$\begin{aligned} m^2 &= \frac{1}{2}\left[-2v^2\lambda_1 - v_\Delta^2(\lambda_4 + \lambda_5) + 2\sqrt{2}\mu v_\Delta\right], \\ M^2 &= M_\Delta^2 - \frac{1}{2}\left[2v_\Delta^2(\lambda_2 + \lambda_3) + v^2(\lambda_4 + \lambda_5)\right], \quad M_\Delta^2 \equiv \frac{v^2\mu}{\sqrt{2}v_\Delta}. \end{aligned} \tag{3}$$

[2] Depending on m_{H^+}, there are the other decay modes, e.g., $H^+ \to hW^+$, $H^+ \to t\bar{b}$, etc..
[3] Recently the importance of this cascade decay has been mentioned in Refs. [12, 13].
[4] There are parameter regions where H^{++} decays into the same sign dilepton even in the case of $\xi \neq 0$ when v_Δ is extremely small. In such a case, the scenario of the triplet-like scalar boson with the mass of $\mathcal{O}(100)$ GeV is excluded by the LHC direct search.

The mass of the doubly-charged scalar bosons $H^{\pm\pm}$ ($=\Delta^{\pm\pm}$) is calculated as

$$\begin{aligned} m^2_{H^{++}} &= M^2_\Delta - v^2_\Delta\lambda_3 - \frac{v^2}{2}\lambda_5 \\ &\simeq M^2_\Delta - \frac{v^2}{2}\lambda_5, \quad (v^2 \gg v^2_\Delta). \end{aligned} \tag{4}$$

Mass eigenstates of the singly-charged states, CP-odd states and CP-even states are obtained by

$$\begin{aligned} &\begin{pmatrix} \varphi^\pm \\ \Delta^\pm \end{pmatrix} = R(\beta_\pm)\begin{pmatrix} w^\pm \\ H^\pm \end{pmatrix}, \quad \begin{pmatrix} \chi \\ \eta \end{pmatrix} = R(\beta_0)\begin{pmatrix} z \\ A \end{pmatrix}, \quad \begin{pmatrix} \varphi \\ \delta \end{pmatrix} = R(\alpha)\begin{pmatrix} h \\ H \end{pmatrix}, \\ &R(\theta) \equiv \begin{pmatrix} \cos\theta & -\sin\theta \\ \sin\theta & \cos\theta \end{pmatrix}, \end{aligned} \tag{5}$$

where $w^\pm$ and z are the Nambu-Goldstone bosons which are absorbed by the longitudeinal mode of $W^\pm$ and Z, respectively. The mixing angles $\beta_\pm$, β_0 and α are expressed as

$$\cos\beta_\pm = \frac{v}{\sqrt{v^2+2v^2_\Delta}}, \quad \cos\beta_0 = \frac{v}{\sqrt{v^2+4v^2_\Delta}}, \quad \tan 2\alpha \simeq \frac{v_\Delta}{v}\frac{4M^2_\Delta - 2v^2(\lambda_4+\lambda_5)}{M^2_\Delta - 2v^2\lambda_1}. \tag{6}$$

The mass formulae for the physical scalar bosons are

$$m^2_{H^+} = M^2_\Delta\left(1+\frac{2v^2_\Delta}{v^2}\right) - \frac{1}{4}(v^2+2v^2_\Delta)\lambda_5 \simeq M^2_\Delta - \frac{v^2}{4}\lambda_5, \tag{7}$$

$$m^2_A = M^2_\Delta\left(1+\frac{4v^2_\Delta}{v^2}\right) \simeq M^2_\Delta, \tag{8}$$

$$\begin{aligned} m^2_H &\simeq M^2_\Delta, \\ m^2_h &\simeq 2\lambda_1 v^2, \end{aligned} \tag{9}$$

for $v^2 \gg v^2_\Delta$. Notice that Eq. (9) is valid as long as $M^2_\Delta > 2\lambda_1 v^2$. Throughout the paper, we keep this relation. From above mass formulae, the mass difference ξ is determined by $-\frac{v^2}{4}\lambda_5$. It is useful to define the mass difference (not squired) as $\Delta m \equiv m_{H^{++}} - m_{H^+}$. In the limit of $v_\Delta \to 0$, Yukawa interactions and gauge interactions of h become completely the same as those of the SM Higgs boson at the tree level. In this sense, we call h the SM-like Higgs boson. Some theoretical bounds for the Higgs potential have been studied in Ref. [21].

The neutrino masses are generated through the Yukawa interaction;

$$\mathcal{L}_\nu = h_{ij}\overline{L^{ic}_L} i\tau_2 \Delta L^j_L + \text{h.c.}, \tag{10}$$

where h_{ij} is a 3×3 symmetric complex matrix and L^i_L is the i-th generation of the left-handed lepton doublet. The neutrino mass matrix is obtained as

$$(\mathcal{M}_\nu)_{ij} = \sqrt{2}h_{ij}v_\Delta = h_{ij}\frac{\mu v^2}{M^2_\Delta}. \tag{11}$$

By this equation, the Yukawa coupling constant h_{ij} and v_Δ are related with each other. This characteristic feature is important to discuss the decay of the triplet-like scalar bosons: $H^{\pm\pm}$, $H^\pm$, H and A. The decay branching fractions of these scalar bosons are discussed in the next section.

In the HTM, the rho parameter ρ is predicted at the tree level as

$$\rho = \frac{1+\frac{2v^2_\Delta}{v^2}}{1+\frac{4v^2_\Delta}{v^2}} \simeq 1 - \frac{2v^2_\Delta}{v^2}, \tag{12}$$

so that v_Δ is constrained from the current experimental data, $\rho_{\rm exp} = 1.0008^{+0.0017}_{-0.0007}$ [22], i.e., $v_\Delta \lesssim 8$ GeV.

We here give some comments on radiative corrections in this model. The relation $m^2_{H^{++}} - m^2_{H^+} \simeq m^2_{H^+} - m^2_{\phi^0}$ can be changed when radiative corrections are taken into account. Radiative corrections in models with $\rho \neq 1$ at the tree level have been studied in Refs. [23–29], where the correction to the rho parameter is mainly discussed. However, such an analysis of the radiative correction has not been done yet for the HTM with the triplet field with $Y = 1$,

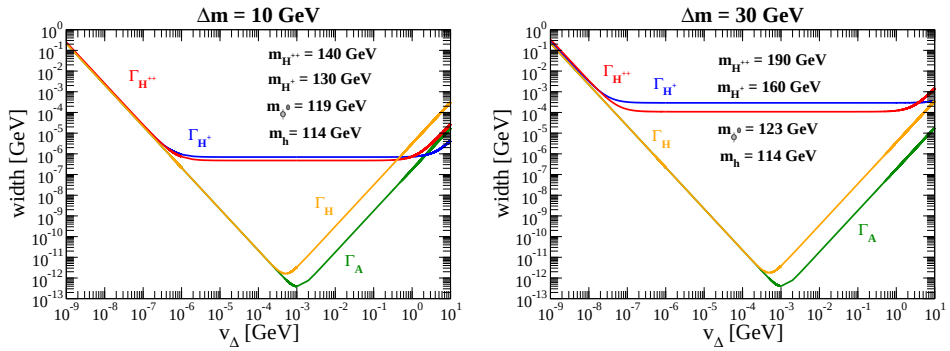

FIG. 1: Decay width of H^{++}, H^+, H and A as a function of v_Δ. We take $m_{H^{++}} = 140$ GeV (190 GeV), Δm =10 GeV (30 GeV) in the left (right) figure. In both the figures, m_h is fixed to be 114 GeV.

neither to the rho parameter nor to the Higgs potential. A detailed study of radiative corrections in the HTM is an important and interesting issue which will be performed in near future. In this paper, we focus on the strategy of measuring the masses of the triplet field in the case with the mass differences at the LHC, so that we do not give a further discussion on the radiative correction. At the one-loop level, the relation in mass differences can be rewritten as

$$\frac{m^2_{H^{++}} - m^2_{H^+}}{m^2_{H^+} - m^2_{\phi^0}} \simeq 1 + \delta_{\phi^0}, \quad (\phi^0 = H \text{ or } A), \tag{13}$$

where δ_{ϕ^0} is the deviation from the tree level prediction due to radiative corrections, which is given as a function of the masses and mixing angles. In principle, we may test the HTM with this kind of the corrected mass relation instead of the tree level formula by measuring the masses of the bosons.

III. DECAY OF THE SCALAR BOSONS

In this section, we discuss the decay branching ratios of the triplet-like scalar bosons $H^{\pm\pm}$, $H^\pm$, H and A [11]. We discuss both the cases of $\xi = 0$ and $\xi > 0$. At the end of this section, we also comment on the case of $\xi < 0$. The decay modes of the triplet-like scalar bosons can be classified into three modes: (i) decay via the Yukawa coupling defined in Eq. (10), (ii) that via v_Δ and (iii) that via the gauge coupling. The magnitude of the Yukawa coupling constant and v_Δ are related from the neutrino mass as in Eq. (11). The main decay modes of H^{++} and H^+ depend on the size of v_Δ and ξ. The decay mode (iii) particularly is important in the case of $\xi \neq 0$. Typically, in this case, the heaviest triplet-like scalar boson decays into the second heaviest one associated with the W boson. The formulae of the decay rates of $H^{\pm\pm}$, $H^\pm$, H and A are listed in Appendix A. Here, the leptonic decay modes through the Yukawa coupling h_{ij} are summed over all flavors and each element of h_{ij} is taken to be 0.1 eV/$(\sqrt{2}v_\Delta)$.

In FIG. 1, the decay width for the triplet-like scalar bosons is shown in the case of $\Delta m = 10$ GeV and $\Delta m = 30$ GeV. Since there is a decay mode through the gauge coupling the minimum value of the decay widths of H^{++} and H^+ are $\mathcal{O}(10^{-6})$ GeV for $\Delta m = 10$ GeV and $\mathcal{O}(10^{-4})$ GeV for $\Delta m = 30$ GeV. On the other hand, the decay widths of H and A become minimum at $v_\Delta \simeq 10^{-4} - 10^{-3}$ GeV with the magnitude of $\mathcal{O}(10^{-13} - 10^{-12})$ GeV. This result is consistent with Ref. [11].

We consider the decay branching ratio of H^{++}. In the case with $\Delta m = 0$ and $m_{H^{++}}$=140 GeV, H^{++} decays into $\ell^+\ell^+$ with $v_\Delta \lesssim 10^{-3}$ GeV or W^+W^+ with $v_\Delta \gtrsim 10^{-3}$ GeV. The value of v_Δ where the main decay mode changes from $H^{++} \to \ell^+\ell^+$ to $H^{++} \to W^+W^+$ is shifted at $v_\Delta \simeq 10^{-4}$ GeV when $m_{H^{++}} = 300$ GeV. In the case of Δm =10 GeV, H^{++} decays into H^+W^{+*} in the region of 10^{-6} GeV $\lesssim v_\Delta \lesssim 1$ GeV (10^{-6} GeV $\lesssim v_\Delta \lesssim 0.1$ GeV) for $m_{H^{++}}$=140 GeV (320 GeV). Similarly, in the case of Δm =30 GeV, H^{++} decays into H^+W^{+*} in the region of 10^{-7} GeV $\lesssim v_\Delta \lesssim 1$ GeV for $m_{H^{++}}$=190 GeV and 360 GeV. In FIG. 2, the decay branching ratio of H^{++} is shown as a function of v_Δ.

The decay branching ratio of H^+ is shown in FIG. 3. In the case of $\Delta m = 0$, H^+ decays into $\ell^+\nu$ with $v_\Delta < 10^{-4} - 10^{-3}$ GeV. When $v_\Delta > 10^{-4} - 10^{-3}$ GeV, H^+ decays into $\tau^+\nu$, W^+Z and $c\bar{s}$ for $m_{H^+} = 120$ GeV, while H^+ decays into $t\bar{b}$, W^+Z and hW^+ for $m_{H^+} = 300$ GeV. In the case of Δm =10 GeV, similarly to the decay of H^{++}, H^+ decays into $\phi^0 W^{+*}$ in the region of 10^{-6} GeV $\lesssim v_\Delta \lesssim 1$ GeV (10^{-6} GeV $\lesssim v_\Delta \lesssim 10^{-2}$ GeV) for $m_{H^+} = 130$

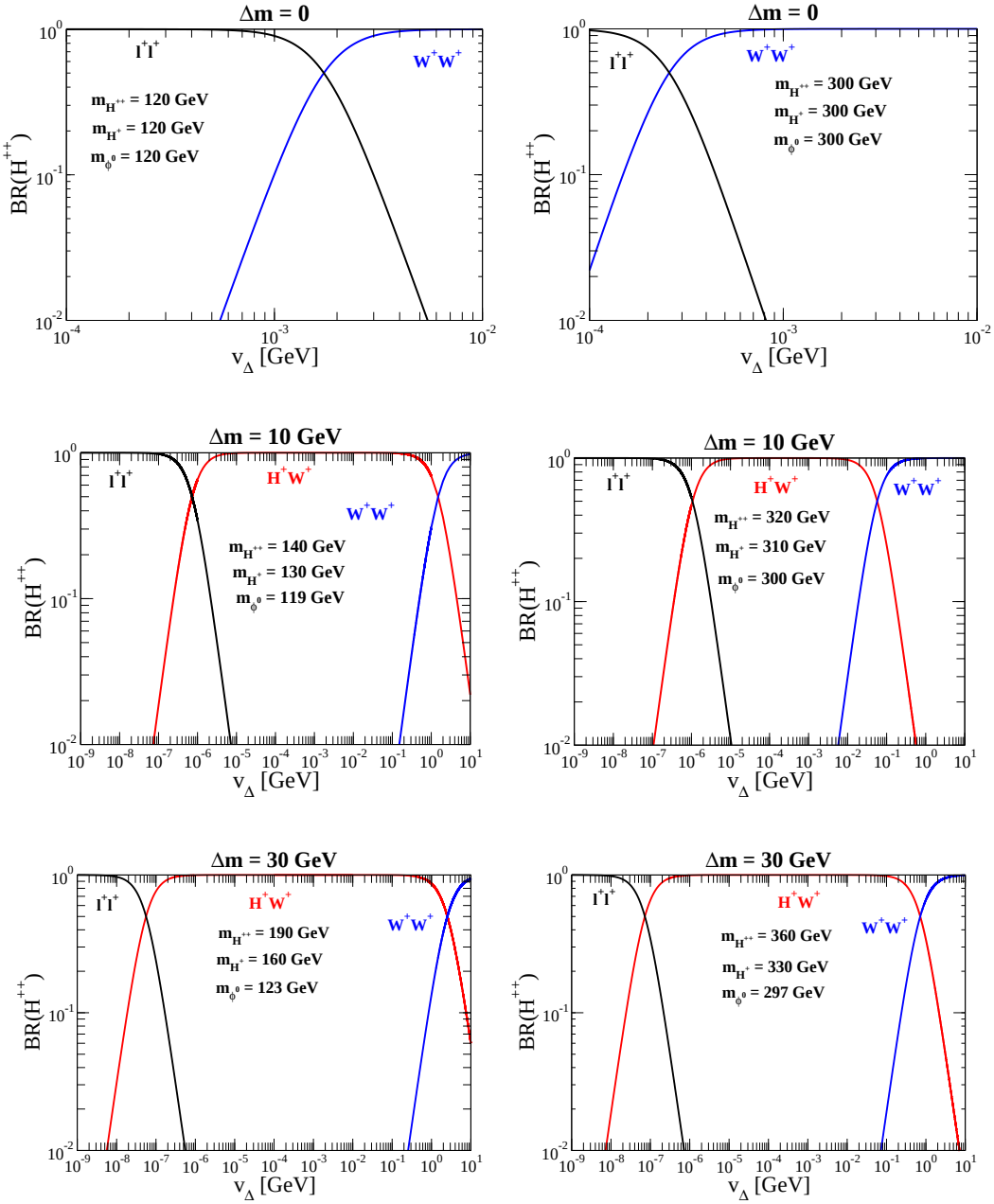

FIG. 2: Decay branching ratio of H^{++} as a function of v_Δ. In the upper left (right) figure, $m_{H^{++}}$ is fixed to be 120 GeV (300 GeV), and Δm is taken to be zero. In the middle left (right) figure, $m_{H^{++}}$ is fixed to be 140 GeV (320 GeV), and Δm is taken to be 10 GeV. In the bottom left (right) figure, $m_{H^{++}}$ is fixed to be 190 GeV (360 GeV), and Δm is taken to be 30 GeV.

GeV (310 GeV). In the case of Δm =30 GeV, H^+ decays into $\phi^0 W^{+*}$ in the region of 10^{-7} GeV $\lesssim v_\Delta \lesssim$ 10 GeV (10^{-7} GeV $\lesssim v_\Delta \lesssim 10^{-1}$ GeV) for $m_{H^+} = 160$ GeV (330 GeV).

The decay branching ratios of H and A are shown in FIG. 4. Both H and A decay into neutrinos in the region of $v_\Delta < 10^{-4} - 10^{-3}$ GeV. When $v_\Delta > 10^{-4} - 10^{-3}$ GeV, both H and A decay into $b\bar{b}$ with $m_{\phi^0} = 119$ GeV while H (A) decay into hh and ZZ (hZ) with $m_{\phi^0} = 300$ GeV.

Finaly, we comment on the case of $\xi < 0$. In this case, H and A can decay into $H^\pm W^{\mp(*)}$ depending on the magnitude of ξ and v_Δ. At the same time, H^+ can decay into $H^{++}W^{-(*)}$. The decay of H^{++} is the same as in the case without the mass difference.

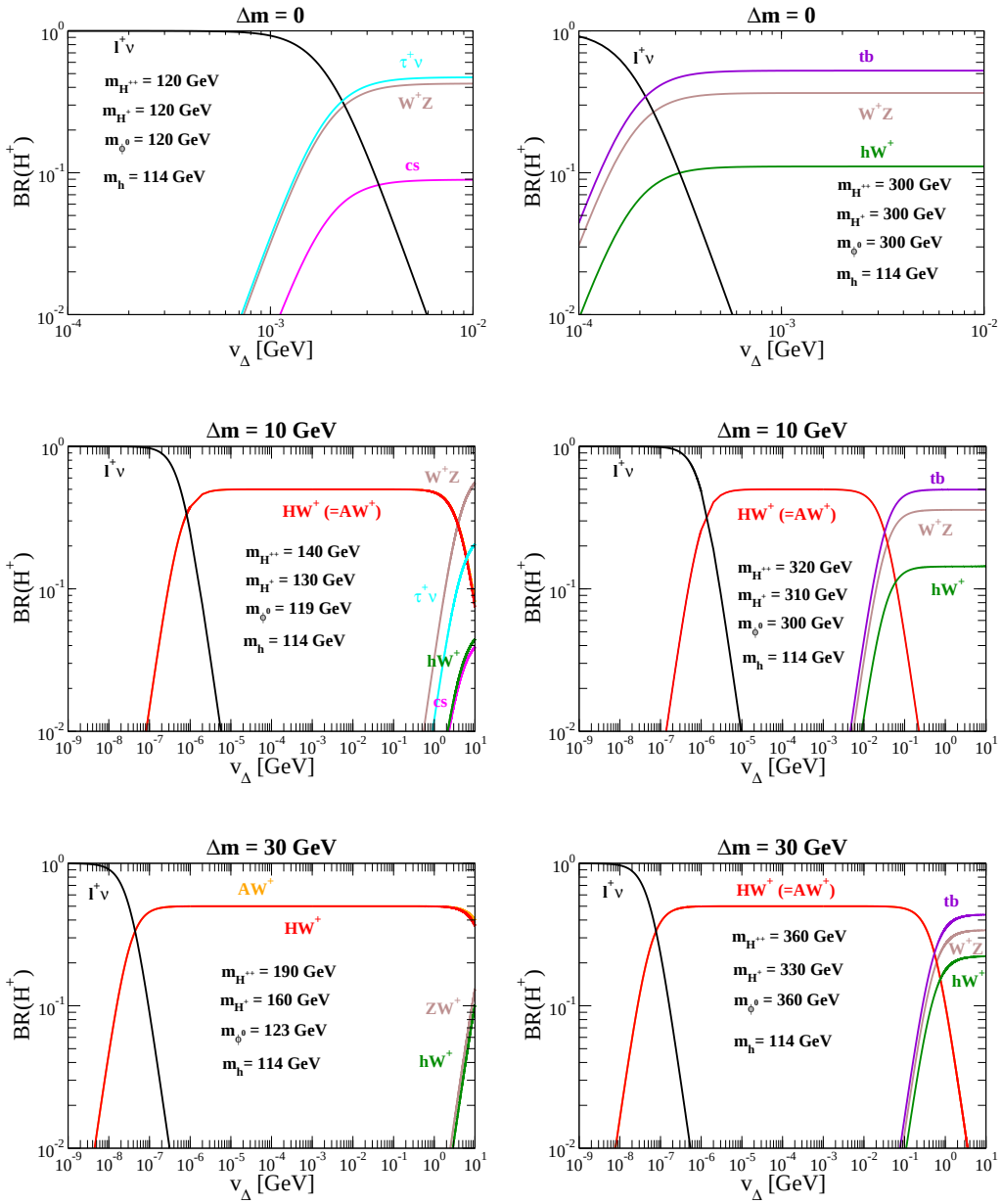

FIG. 3: Decay branching ratio of H^+ as a function of v_Δ. In all the figures, m_h is taken to be 114 GeV. In the upper left (right) figure, m_{H^+} is fixed to be 120 GeV (300 GeV), and Δm is taken to be zero. In the middle left (right) figure, m_{H^+} is fixed to be 130 GeV (310 GeV), and Δm is taken to be 10 GeV. In the bottom left (right) figure, m_{H^+} is fixed to be 160 GeV (330 GeV), and Δm is taken to be 30 GeV.

IV. MASS DETERMINATION OF THE TRIPLET-LIKE SCALAR BOSONS AT THE LHC

In this section, we discuss how the HTM with $\xi > 0$ can be tested at the LHC. At the LHC, the triplet-like scalar bosons $H^{\pm\pm}$, $H^\pm$, H and A are mainly produced through the Drell-Yan processes, for instance, $pp \to H^{++}H^{--}$, $pp \to H^+H^-$, $pp \to H^{\pm\pm}H^\mp$ and $pp \to H^\pm\phi^0$ and $pp \to HA$. In particular, latter three processes are important when we consider the case of $\xi > 0$. The cross sections for the latter three production processes are shown in FIG. 5.

We comment on vector boson fusion production processes. There are two types of the vector boson fusion processes. First one is the process via $VV\Delta$ vertices, where $V = Z$ or $W^\pm$. The cross section of this process is small, since the

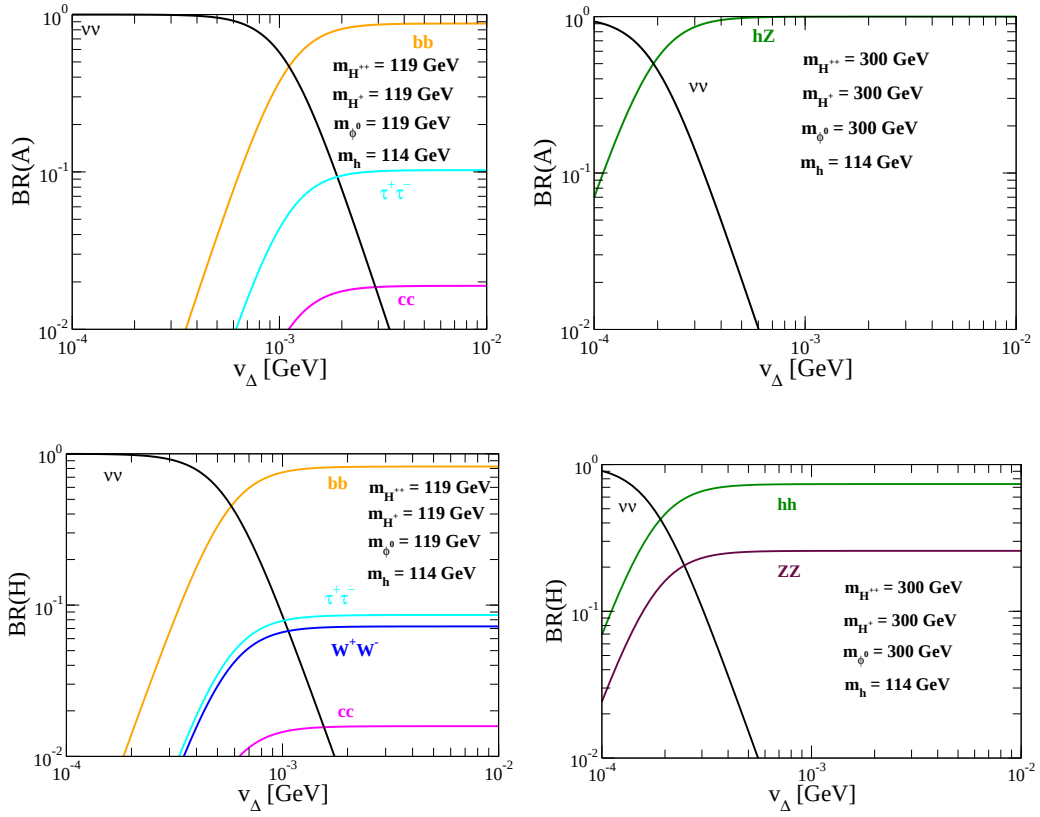

FIG. 4: Decay branching ratios of A and H as a function of v_Δ. In all the figures, m_h is taken to be 114 GeV. In the upper left (right) figure, the branching ratio of A is shown in the case of $m_A = 119$ GeV (300 GeV). In the lower left (right) figure, the branching ratio of H is shown in the case of $m_H = 119$ GeV (300 GeV).

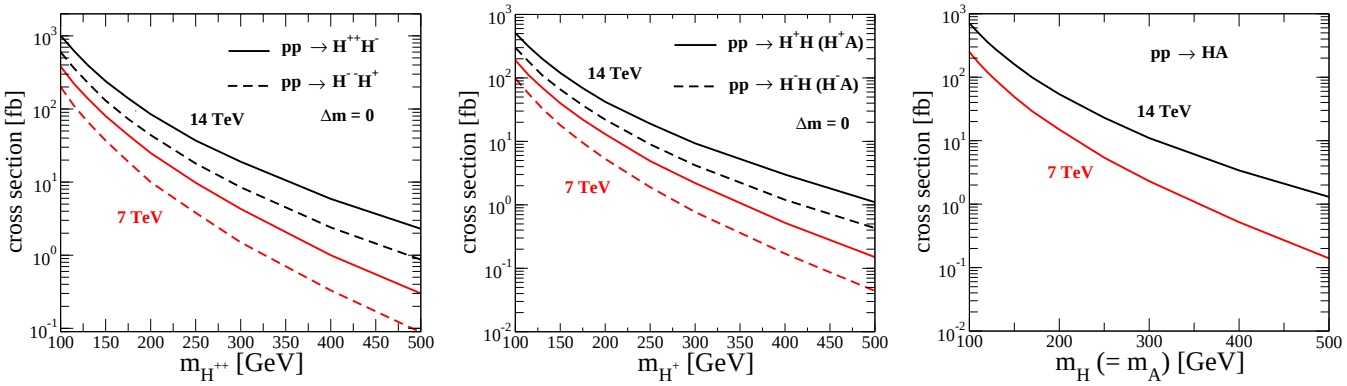

FIG. 5: Production cross sections for the triplet-like scalar bosons in the Drell-Yan process.

$VV\Delta$ vertex is proportional to v_Δ [5]. The other one is the process via the gauge coupling constant. In particular, $qq \to q'q'H^{++}\phi^0$ is the unique process whose difference of the electric charge between produced scalar bosons is two. This production cross section is 0.51 fb (0.13 fb) at $\sqrt{s} = 14$ TeV ($\sqrt{s} = 7$ TeV) assuming mass parameters Set 1

[5] The magnitude of v_Δ may be determined indirectly via B_{ee}/B_{WW} or Γ_{ee} and $0\nu\beta\beta$ where $H^{++} \to \ell^+\ell^+$, W^+W^+ are dominant [15]. On the other hand, it could be directly measured via $qq \to q'qW^{\pm *}Z^* \to q'qH^\pm$ at the LHC [30] and via $e^+e^- \to Z^* \to H^\pm W^\mp$ at the ILC [31].

Process	$\Delta m = 0$ at $\sqrt{s} = 14$ TeV (7 TeV)	Δm =10 GeV at $\sqrt{s} = 14$ TeV (7 TeV)	Δm =30 GeV at $\sqrt{s} = 14$ TeV (7 TeV)
$pp \to H^{++}H^-$	310 fb (110 fb)	350 fb (120 fb)	140 fb (43 fb)
$pp \to H^+H$	150 fb (53 fb)	230 fb (81 fb)	150 fb (50 fb)
$pp \to HA$	200 fb (65 fb)	370 fb (130 fb)	330 fb (110 fb)

TABLE I: Production cross sections for the triplet-like scalar bosons in the case of $\Delta m = 0$ with $m_{H^{++}} = 140$ GeV, those of the case for Set 1 and Set 2.

Scenario	Decay of H^{++}	Decay of H^+	Decay of H	Decay of A
(1a) ($v_\Delta = 5$ GeV)	W^+W^{+*} [0.93]	$W^{+*}Z$ [0.37], $\tau^+\nu$ [0.14]	$b\bar{b}$ [0.82]	$b\bar{b}$ [0.89]
(1b) ($v_\Delta = 10^{-2}$ GeV)	H^+W^{+*} [1.0]	AW^{+*} [0.5], HW^{+*} [0.5]	$b\bar{b}$ [0.82]	$b\bar{b}$ [0.89]
(1c) ($v_\Delta = 10^{-5}$ GeV)	H^+W^{+*} [1.0]	AW^{+*} [0.5], HW^{+*} [0.5]	$\nu\nu$ [1.0]	$\nu\nu$ [1.0]
(1d) ($v_\Delta = 10^{-8}$ GeV)	$\ell^+\ell^+$ [1.0]	$\ell^+\nu$ [1.0]	$\nu\nu$ [1.0]	$\nu\nu$ [1.0]

TABLE II: The main decay mode of the triplet-like scalar bosons in Scenario (1a) to Scenario (1d). The masses of the triplet-like scalar bosons are taken to be as for Set 1. The number in ( ) represents the sample value of v_Δ corresponding to the scenario. The number in [ ] represents the value of the decay branching ratio corresponding to the value of v_Δ displayed in ( ) in the same row. Here, $\ell\ell$ mode and $\ell\nu$ mode are summed over all flavors.

which is given just below.

We consider the following two sets for mass parameters:

$$\begin{aligned}
&\text{(Set 1)} \quad m_{H^{++}} = 140 \text{ GeV}, \quad m_{H^+} = 130 \text{ GeV}, \quad m_H = m_A = 119 \text{ GeV}, \quad m_h = 114 \text{ GeV}, \\
&\text{(Set 2)} \quad m_{H^{++}} = 190 \text{ GeV}, \quad m_{H^+} = 160 \text{ GeV}, \quad m_H = m_A = 123 \text{ GeV}, \quad m_h = 114 \text{ GeV},
\end{aligned}$$

which correspond to the cases with ξ=(52 GeV)^2 and ξ=(102 GeV)^2, respectively. In the following numerical analysis, $\lambda_2 = 0$ is taken. In these parameter sets, the production cross sections for the triplet-like scalar bosons are listed in TABLE I. We can classify scenarios by the following four regions of v_Δ for Set 1:

$$\begin{aligned}
&\text{Scenario (1a)} \quad v_\Delta \gtrsim 1 \text{ GeV}, \\
&\text{Scenario (1b)} \quad 10^{-3} \text{ GeV} \lesssim v_\Delta \lesssim 1 \text{ GeV}, \\
&\text{Scenario (1c)} \quad 10^{-6} \text{ GeV} \lesssim v_\Delta \lesssim 10^{-3} \text{ GeV}, \\
&\text{Scenario (1d)} \quad v_\Delta \lesssim 10^{-6} \text{ GeV}.
\end{aligned}$$

We can also classify scenarios by the following four regions of v_Δ for Set 2:

$$\begin{aligned}
&\text{Scenario (2a)} \quad v_\Delta \gtrsim 1 \text{ GeV}, \\
&\text{Scenario (2b)} \quad 10^{-4} \text{ GeV} \lesssim v_\Delta \lesssim 1 \text{ GeV}, \\
&\text{Scenario (2c)} \quad 10^{-7} \text{ GeV} \lesssim v_\Delta \lesssim 10^{-4} \text{ GeV}, \\
&\text{Scenario (2d)} \quad v_\Delta \lesssim 10^{-7} \text{ GeV}.
\end{aligned}$$

In each scenario, main decay modes of the triplet-like scalar bosons are listed in TABLE II and TABLE III. We here analyse the signal for Set 1 which may be used to reconstruct the masses of the triplet-like scalar bosons. The signal distributions discussed below are calculated by using CalcHEP [32].

Scenario (1a) ;

We can measure $m_{H^{++}}$ by observing the endpoint in the transverse mass distribution of the $\ell^+\ell^+\not{E}_T$ system in the process $pp \to H^{++}H^- \to (W^{+*}W^+)(W^{-*}Z) \to (\ell^+\ell^+\not{E}_T)(jjjj)$, (FIG. 6 upper left). At the same time, we can also determine m_{H^+} by measuring the endpoint in the transverse mass distribution of the $\ell^+jj\not{E}_T$ system or the $\ell^+\not{E}_T$ system in the process $pp \to H^+\phi^0 \to (W^{+*}Z)(b\bar{b}) \to (\ell^+jj\not{E}_T)(j_bj_b)$ or $pp \to H^+\phi^0 \to (\tau^+\nu)(b\bar{b}) \to (\ell^+\not{E}_T)(j_bj_b)$, (FIG. 6 upper right and lower left). In addition, m_{ϕ^0} can be determined by using the invariant mass distribution or by observing the endpoint in the transverse mass distribution of the $b\bar{b}$ system in the process $pp \to HA \to (b\bar{b})(b\bar{b}) \to (j_bj_b)(j_bj_b)$, (FIG. 6 lower right).

Scenario (1b) ;

We can determine $m_{H^{++}}$ by measuring the endpoint in the transverse mass distribution of the $\ell^+\ell^+j_bj_b\not{E}_T$ system in the process $pp \to H^{++}H^- \to (W^{+*}W^{+*}b\bar{b})(W^{-*}b\bar{b}) \to (\ell^+\ell^+j_bj_b\not{E}_T)(jjj_bj_b)$, (FIG. 7 left). Analysing

Scenario	Decay of H^{++}	Decay of H^+	Decay of H	Decay of A
(2a) [$v_\Delta = 5$ GeV]	W^+W^{+*} [0.76]	AW^{+*} [0.47] HW^{+*} [0.46]	$b\bar{b}$ [0.78]	$b\bar{b}$ [0.89]
(2b) [$v_\Delta = 10^{-2}$ GeV]	H^+W^{+*} [1.0]	AW^{+*} [0.5] HW^{+*} [0.5]	$b\bar{b}$ [0.78]	$b\bar{b}$ [0.89]
(2c) [$v_\Delta = 10^{-5}$ GeV]	H^+W^{+*} [1.0]	AW^{+*} [0.5] HW^{+*} [0.5]	$\nu\nu$ [1.0]	$\nu\nu$ [1.0]
(2d) [$v_\Delta = 10^{-8}$ GeV]	$\ell^+\ell^+$ [0.97]	$\ell^+\nu$ [0.91]	$\nu\nu$ [1.0]	$\nu\nu$ [1.0]

TABLE III: The main decay mode of the triplet-like scalar bosons in Scenario (2a) to Scenario (2d). The masses of the triplet-like scalar bosons are taken to be as for Set 2. The number in ( ) represents the sample value of v_Δ corresponding to the scenario. The number in [ ] represents the value of the decay branching ratio corresponding to the value of v_Δ displayed in ( ) in the same row. Here, $\ell\ell$ mode and $\ell\nu$ mode are summed over all flavors.

	$m_{H^{++}}$	m_{H^+}	m_H/m_A
(1a)	$pp \to H^{++}H^- \to (\ell^+\ell^+\not{E}_T)(jjjj)$ [2.8 fb] (0.95 fb)	$pp \to H^+H \to (\ell^+jj\not{E}_T)(j_bj_b)$ [11 fb] (3.8 fb) $pp \to H^+H \to (\ell^+\not{E}_T)(j_bj_b)$ [9.3 fb] (3.3 fb)	$pp \to HA \to (j_bj_b)(j_bj_b)$ [270 fb] (95 fb) $pp \to H^+H \to (\ell^+\not{E}_T)(j_bj_b)$ [9.3 fb] (3.3 fb)
(1b)	$pp \to H^{++}H^- \to (\ell^+\ell^+j_bj_b\not{E}_T)(jjj_bj_b)$ [8.4 fb] (2.9 fb)	$pp \to H^+H \to (\ell^+j_bj_b\not{E}_T)(j_bj_b)$ [36 fb] (13 fb)	$pp \to HA \to (j_bj_b)(j_bj_b)$ [270 fb] (95 fb) $pp \to H^+H \to (\ell^+j_bj_b\not{E}_T)(j_bj_b)$ [36 fb] (13 fb)
(1c)	Challenging		
(1d)	Excluded		

TABLE IV: The processes which can be used to reconstruct the masses of the triplet-like scalar bosons are summarized. The numbers in [ ] and ( ) represent the cross section for the final state of the process at $\sqrt{s} = 14$ TeV and $\sqrt{s} = 7$ TeV, respectively, for Set 1. The values of the decay branching ratios of the triplet-like scalar bosons are listed in TABLE II. In this table, the b-tagging efficiency is assumed to be 100 %.

the transverse mass distribution for the $\ell^+\ell^+j_bj_b\not{E}_T$ system, we treat that a lepton pair $\ell^+\nu$ from W^{+*} as one massless fermion as represented X^+ in FIG. 7. This procedure is justified since the angle between ℓ^+ and ν is distributed almost around 0°. We can also determine m_{H^+} by measuring the endpoint in the transverse mass distribution of the $\ell^+j_bj_b\not{E}_T$ system in the process $pp \to H^+\phi^0 \to (W^{+*}b\bar{b})(b\bar{b}) \to (\ell^+j_bj_b\not{E}_T)(j_bj_b)$, (FIG. 7 center). In addition, m_{ϕ^0} can be reconstructed by measuring the invariant mass distribution of the $b\bar{b}$ system and by observing the endpoint of the transverse mass distribution of the $b\bar{b}$ system in the process $pp \to HA \to (b\bar{b})(b\bar{b}) \to (j_bj_b)(j_bj_b)$ (FIG. 7 right).

Scenario (1c) ;
The final state of the decay of the triplet-like scalar bosons always include neutrinos, so that the reconstruction of the masses of the triplet-like scalar bosons would be challenging.

Scenario (1d) ;
This scenario is already excluded from the direct search results at the LHC for the processes of $pp \to H^{++}H^{--}(H^{\pm\pm}H^{\mp}) \to \ell^+\ell^+\ell^-\ell^-(\ell^\pm\ell^\pm\ell^\mp\nu)$.

In TABLE IV, processes which can use the reconstruction of the masses of the triplet-like scalar bosons are summarized in each scenario. The cross sections for the final states of each process are also listed. In the case of Set 2, the masses of the triplet like scalar bosons may be able to reconstruct in the similar way to the case of Set 1. Thus, we show only the signal cross sections for the final states for Set 2 in TABLE V.

V. DISCUSSIONS

We give comments on the discrimination of the model from the others which contain doubly-charged scalar bosons such as that from $Y = 2$ singlet scalar fields and/or $Y = 3/2$ doublet scalar fields. First, doubly-charged scalar

	$m_{H^{++}}$	m_{H^+}	m_H/m_A
(2a)	$pp \to H^{++}H^- \to (\ell^+\ell^+\not{E}_T)(jjj_bj_b)$ [2.7 fb] (0.84 fb)	$pp \to H^+H \to (\ell^+j_bj_b\not{E}_T)(j_bj_b)$ [21 fb] (6.9 fb)	$pp \to HA \to (j_bj_b)(j_bj_b)$ [230 fb] (76 fb)
(2b)	$pp \to H^{++}H^- \to (\ell^+\ell^+j_bj_b\not{E}_T)(jjj_bj_b)$ [3.2 fb] (0.99 fb)	$pp \to H^+H \to (\ell^+j_bj_b\not{E}_T)(j_bj_b)$ [22 fb] (7.2 fb)	$pp \to HA \to (j_bj_b)(j_bj_b)$ [230 fb] (76 fb)
(2c)	Challenging		
(2d)	Excluded		

TABLE V: The processes which can be used to reconstruct the masses of the triplet-like scalar bosons are summarized. The numbers in [ ] and ( ) represent the cross section for the final state of the process at $\sqrt{s} = 14$ TeV and $\sqrt{s} = 7$ TeV, respectively, for Set 2. The values of the decay branching ratios of the triplet-like scalar bosons are listed in TABLE III. In this table, the b-tagging efficiency is assumed to be 100 %.

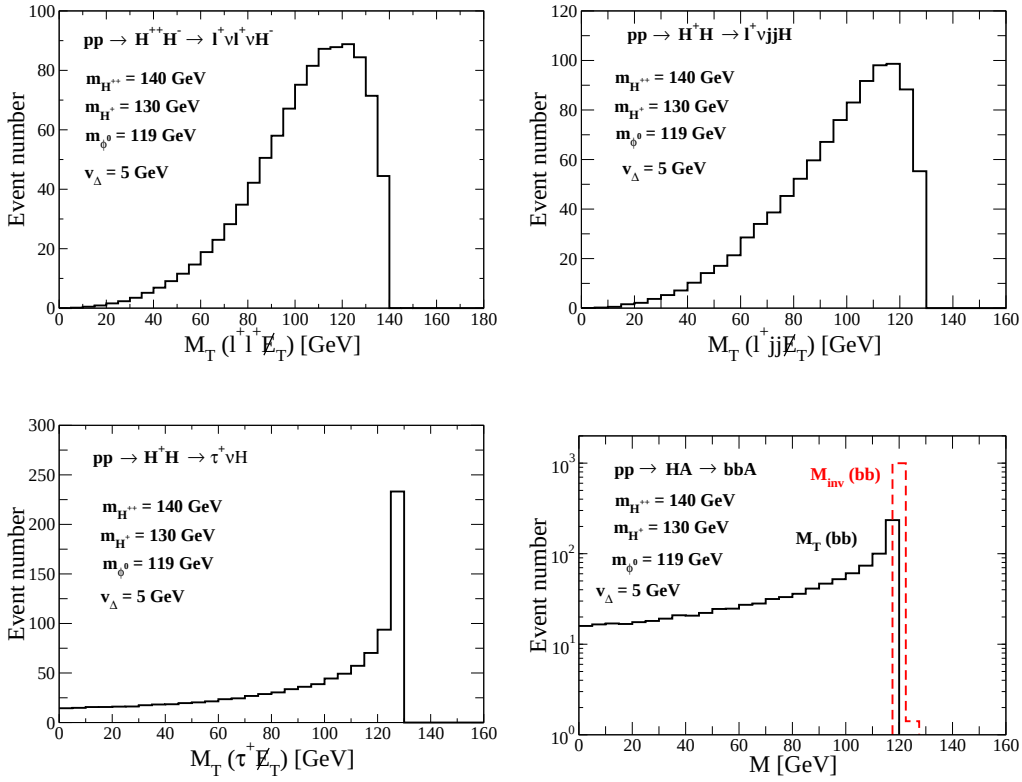

FIG. 6: The transvers mass distributions for each system in Scenario (1a). The total event number is assumed to be 1000. In the bottom-right figure, the horizontal axis M represents the transverse mass distribution for the $b\bar{b}$ system $M_T(bb)$ (solid) or the invariant mass distribution for the $b\bar{b}$ system $M_{\rm inv}(bb)$ (dashed).

bosons from singlet fields appear in the Zee-Babu model [18] which generates neutrino masses at the 2-loop level. The doubly-charged scalar bosons from this model do not couple to W boson. Thus, it may be distinguished by the production process for doubly-charged scalar bosons associated with singly-charged scalar bosons. Second, we consider the discrimination of the HTM from the model with the $Y = 3/2$ doublet $H_{3/2} = (H^{++}_{3/2}, H^+_{3/2})$. The doubly-charged component field $H^{++}_{3/2}$ decays into $H^+_{3/2}W^{+(*)}$ because $H_{3/2}$ does not receive the VEV as discussed in Ref. [19] [6]. $H^+_{3/2}$

[6] If higher order operators are introduced as discussed in Refs. [8, 20], $H^{++}_{3/2}$ can decay into the same sign dilepton.

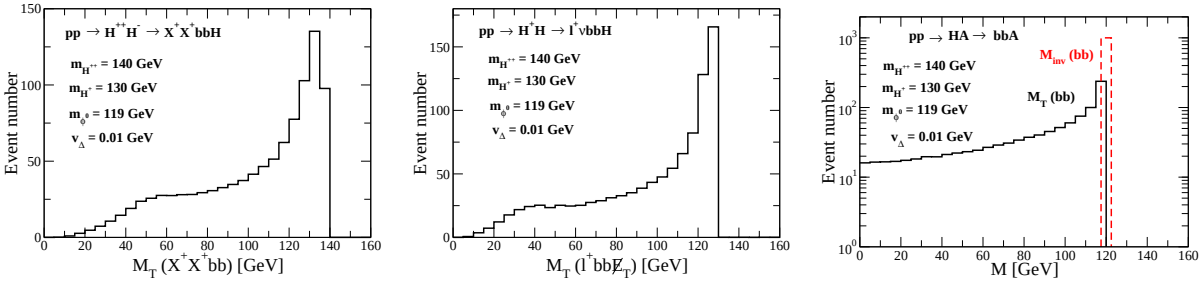

FIG. 7: The transvers mass distributions for each system in Scenario (1b). The total event number is assumed to be 1000. In the right figure, the horizontal axis M represents the transverse mass distribution for the $b\bar{b}$ system $M_T(bb)$ (solid) or the invariant mass distribution for the $b\bar{b}$ system $M_{\rm inv}(bb)$ (dashed).

decays into $\tau^+\nu$ or cs via the mixing with the singly-charged scalar boson from the $Y = 1/2$ doublet fields [7] while H^+ decays into $\phi^0 W^{+(*)}$ in the HTM. Therefore, we can distinguish these models because the final state is different. Finally, the singly-charged Higgs boson in the HTM can also be discriminated from that in the two Higgs doublet model (THDM). In both the models H^+ is produced via $pp \to W^{+*} \to H^+ A$ ($H^+ H$). In the THDM with the type II Yukawa interaction including the minimal supersymmetric standard model [8], H^+ decays into $\tau^+\nu$ or $t\bar{b}$ depending on the mass of the H^+ while H or A decays into $b\bar{b}$ as long as the masses are not too heavy. Therefore, the final state of the $pp \to H^+ A$ is $\tau^+\nu b\bar{b}$ or $W^+ b\bar{b}b\bar{b}$ in the type II THDM [34]. Although the latter final state is the same as that in the HTM with $\xi > 0$ we may be able to distinguish these models by reconstructing the top quark in the $W^+ b$ system. In the THDM with the type X Yukawa interaction (the lepton specific THDM), extra neutral Higgs bosons decay into $\tau^+\tau^-$ instead of $b\bar{b}$ [35], which is different from the HTM, and we would be able to separate the models.

We have discussed the case of light triplet-like scalar bosons with these masses of $\mathcal{O}$ (100) GeV. Here, we comment on a rather heavy triplet-like scalar bosons case, e.g., $m_{H^{++}}$= 320 GeV, m_{H^+}= 310 GeV and m_{ϕ^0}= 300 GeV. The biggest change should be in the decay of the neutral scalar bosons; i.e., H (A) decays into hh (hZ) when $v_\Delta \gtrsim 10^{-3}$ GeV (see FIG. 4). Decay of H^{++} is almost the same as in the case of the light triplet-like scalar bosons case (see FIG. 2). H^+ can decay into $t\bar{b}$ instead of $\tau^+\nu$ (see FIG. 3). Since decay modes of the neutral scalar bosons change, final states via H or A include more jets. At the same time, the production cross sections for the Drell-Yan processes decrease in this case. For instance, the cross sections for $pp \to H^{++}H^-$, $pp \to H^+\phi^0$ and $pp \to HA$ are 15 fb (3.4 fb), 7.7 fb (1.7 fb) and 5.6 fb (1.1 fb), respectively at $\sqrt{s} = 14$ TeV (7 TeV). Therefore, measurement the masses of the triplet-like scalar bosons is rather challenging, especially when H^{++} decays into $H^+ W^{+(*)}$.

In this paper, we only have discussed the signal processes and we have not discussed backgrounds against the signal. The background analysis is beyond the scope in this paper. It would be expected that the backgrounds can be reduced after the appropriate kinematic cuts. For example, in the case of Scenario (1b), the main background against the signal $pp \to H^{++}H^- \to (\ell^+\ell^+ b\bar{b}\not{E}_T)(jjb\bar{b})$ may come from $t\bar{t}W^+W^-$. Typically, the cross section for this background is $\mathcal{O}(1)$ pb at $\sqrt{s} = 14$ TeV. In the case where one of the W boson from the top quark decays hadronicaly; i.e., $t\bar{t}W^+W^- \to (b\ell^+\nu)(\bar{b}jj)(\ell^+\nu)(jj)$, the cross section for the final state of the background would be $\mathcal{O}(10)$ fb. On the other hand, the cross section for the final state of the signal $pp \to H^{++}H^- \to (\ell^+\ell^+ b\bar{b}\not{E}_T)(jjb\bar{b})$ is 8.4 fb at $\sqrt{s} = 14$ TeV. Although the cross sections for the signal and the background are comparable at this stage, the background can be further reduced by reconstructing the top quarks by using the invariant mass distribution of the bjj system and the endpoint in the transverse mass distribution of the $b\ell\not{E}_T$ system. In the case where both the W bosons from the top quarks decay leptonicaly; i.e., $t\bar{t}W^+W^- \to (b\ell^+\nu)(\bar{b}\ell^-\nu)(jj)(jj)$, the reconstruction of the top quarks would be difficult. However, by using the electric charge identification for leptons, the background and the signal can be further separated. The main backgrounds against the signal $pp \to H^+\phi^0 \to (\ell^+ b\bar{b}\not{E}_T)(b\bar{b})$ may come from $t\bar{t}$ and $t\bar{t}\gamma^*/t\bar{t}g^*$ whose cross sections would be $\mathcal{O}(10)$ pb and $\mathcal{O}(1)$ pb at $\sqrt{s} = 14$ TeV, respectively. The cross section for the final state of the signal $pp \to H^+\phi^0 \to (\ell^+ b\bar{b}\not{E}_T)(b\bar{b})$ is 36 fb at $\sqrt{s} = 14$ TeV. For the background of $t\bar{t} \to (b\ell^+\nu)(\bar{b}jj)$, the top quarks can be reconstructed similarly in the case of the background of $t\bar{t}W^+W^- \to (b\ell^+\nu)(\bar{b}jj)(\ell^+\nu)(jj)$, so that this background would be separated. Next, the process $t\bar{t}\gamma^*/t\bar{t}g^* \to (b\ell^+\nu)(\bar{b}\ell^-\nu)(jj)$ can be a background if one of the charged lepton is miss identified. The cross section for the final state of the background would be $\mathcal{O}(10)$

[7] $H^+_{3/2}$ can decay into the SM particles if the model has two Higgs doublet fields with $Y = 1/2$ at least.
[8] The mass of $H^\pm$ with $\mathcal{O}(100)$ GeV is highly constrained by the $b \to s\gamma$ experiments [33] in the general type II THDM.

fb when the miss-identification rate for a charged lepton is assumed to be 10%. The cross sections for the signal and the background are comparable at this stage. In this case, although we may not be able to use the top quark reconstruction, by using the b-tagging and the cuts for the low energy jet, the background would be expected to be reduced. However, it goes without saying that the detector level simulation is necessary to clarify the feasibility of the signal. This would be a future task.

VI. CONCLUSIONS

In the HTM, a characteristic mass spectrum $\xi = m^2_{H^{++}} - m^2_{H^+} \simeq m^2_{H^+} - m^2_{\phi^0}$ is predicted when $v_\Delta \ll v$. Therefore, by measuring this mass spectrum of the triplet-like scalar bosons, the model can be tested at the LHC. We have investigated the collider signature in the HTM with $\xi > 0$ at the LHC. In this case, H^{++} is the heaviest of all the triplet-like scalar bosons. When $v_\Delta > 10^{-4} - 10^{-3}$ GeV, H^{++} does not decay into the same sign dilepton so that the limit of the mass of H^{++} from the recent results at the LHC cannot be applied. We thus mainly have discussed the case of light triplet-like scalar bosons whose masses are of $\mathcal{O}(100)$ GeV. In such a case, triplet-like scalar bosons mainly decay into $H^{++} \to H^+ W^{+(*)}$, $H^+ \to \phi^0 W^{+(*)}$ and $\phi^0 \to b\bar{b}$. We have found that all the masses of the triplet-like scalar bosons may be able to be reconstructed by measuring the endpoint in the transverse mass distribution and the invariant mass distribution of the systems which are produced via the decay of the triplet-like scalar bosons.

Detector level simulation should be necessary to clarify the feasibility of measuring the masses of the triplet-like scalar bosons.

Acknowledgments The authors would like to thank Hiroaki Sugiyama for a useful comment. The work of M.A. was supported in part by Grant-in-Aid for Scientific Research, No. 22740137. The work of S.K. was supported in part by Grant-in-Aid for Scientific Research, Nos. 22244031 and 23104006. K.Y. was supported by Japan Society for the Promotion of Science.

Appendix A: Decay rates of the triplet-like scalar bosons

In this Appendix, we list the formulae of decay rates for $H^{\pm\pm}$, $H^\pm$, H and A in order.

1. Decay rates of $H^{\pm\pm}$

The decay rates for $H^{\pm\pm}$ can be evaluated as

$$\Gamma(H^{\pm\pm} \to \ell_i^\pm \ell_j^\pm) = S_{ij}|h_{ij}|^2 \frac{m_{H^{++}}}{4\pi}\left(1 - \frac{m_i^2}{m^2_{H^{++}}} - \frac{m_j^2}{m^2_{H^{++}}}\right)\left[\lambda\left(\frac{m_i^2}{m^2_{H^{++}}}, \frac{m_j^2}{m^2_{H^{++}}}\right)\right]^{1/2}, \tag{A1}$$

$$\Gamma(H^{\pm\pm} \to W^\pm W^\pm) = \frac{g^4 v_\Delta^2 m^3_{H^{++}}}{16\pi m_W^4}\left(\frac{3m_W^4}{m^4_{H^{++}}} - \frac{m_W^2}{m^2_{H^{++}}} + \frac{1}{4}\right)\beta\left(\frac{m_W^2}{m^2_{H^{++}}}\right), \tag{A2}$$

$$\Gamma(H^{\pm\pm} \to H^\pm W^\pm) = \frac{g^2 m^3_{H^{++}}}{16\pi m_W^2}\cos^2\beta_\pm\left[\lambda\left(\frac{m_W^2}{m^2_{H^{++}}}, \frac{m^2_{H^+}}{m^2_{H^{++}}}\right)\right]^{3/2}, \tag{A3}$$

$$\Gamma(H^{\pm\pm} \to W^\pm W^{\pm *}) = \frac{3g^6 m_{H^{++}}}{512\pi^3}\frac{v_\Delta^2}{m_W^2}F\left(\frac{m_W^2}{m^2_{H^{++}}}\right), \tag{A4}$$

$$\Gamma(H^{\pm\pm} \to H^\pm W^{\pm *}) = \frac{9g^4 m_{H^{++}}}{128\pi^3}\cos^2\beta_\pm G\left(\frac{m^2_{H^+}}{m^2_{H^{++}}}, \frac{m_W^2}{m^2_{H^{++}}}\right), \tag{A5}$$

where m_i is the lepton mass ($i = e, \mu$ or τ) and $S_{ij} = 1$, (1/2) for $i \neq j$, ($i = j$). The functions of $\lambda(x, y)$, $\beta(x)$, $F(x)$ and $G(x, y)$ are

$$\lambda(x,y) = 1 + x^2 + y^2 - 2xy - 2x - 2y, \tag{A6}$$

$$\beta(x) = \sqrt{\lambda(x,x)} = \sqrt{1-4x}, \tag{A7}$$

$$F(x) = -|1-x|\left(\frac{47}{2}x - \frac{13}{2} + \frac{1}{x}\right) + 3(1-6x+4x^2)|\log\sqrt{x}| + \frac{3(1-8x+20x^2)}{\sqrt{4x-1}}\arccos\left(\frac{3x-1}{2x^{3/2}}\right), \tag{A8}$$

$$\begin{aligned} G(x,y) = \frac{1}{12y}\Bigg\{ & 2\left(-1+x\right)^3 - 9\left(-1+x^2\right)y + 6\left(-1+x\right)y^2 \\ & + 6\left(1+x-y\right)y\sqrt{-\lambda(x,y)}\left[\arctan\left(\frac{-1+x-y}{\sqrt{-\lambda(x,y)}}\right) + \arctan\left(\frac{-1+x+y}{\sqrt{-\lambda(x,y)}}\right)\right] \\ & - 3\left[1+(x-y)^2-2y\right]y\log x\Bigg\}. \end{aligned} \tag{A9}$$

Although the expression in Eq. (A9) is different from that in Ref. [36], we have confirmed that the numerical value by using Eq. (A9) coincides with that by using CalcHEP.

2. Decay rates of $H^\pm$

The decay rates for $H^\pm$ can be evaluated as

$$\begin{aligned} \Gamma(H^\pm \to q\bar{q}') = \frac{3m_{H^+}^3}{8\pi v^2}\sin^2\beta_\pm & \left[\left(\frac{m_q^2}{m_{H^+}^2} + \frac{m_{q'}^2}{m_{H^+}^2}\right)\left(1 - \frac{m_q^2}{m_{H^+}^2} - \frac{m_{q'}^2}{m_{H^+}^2}\right) - 4\frac{m_q^2}{m_{H^+}^2}\frac{m_{q'}^2}{m_{H^+}^2}\right] \\ & \times\left[\lambda\left(\frac{m_q^2}{m_{H^+}^2}, \frac{m_{q'}^2}{m_{H^+}^2}\right)\right]^{1/2}, \end{aligned} \tag{A10}$$

$$\Gamma(H^\pm \to \ell_i^\pm \nu_j) = \delta_{ij}\frac{m_i^2 m_{H^+}}{8\pi v^2}\sin^2\beta_\pm\left(1 - \frac{m_i^2}{m_{H^+}^2}\right)^2 + |h_{ij}|^2\frac{m_{H^+}}{8\pi}\cos^2\beta_\pm\left(1 - \frac{m_i^2}{m_{H^+}^2}\right)^2, \tag{A11}$$

$$\Gamma(H^\pm \to W^\pm Z) = \frac{g^2 g_Z^2}{32\pi m_{H^+}}v_\Delta^2\cos^2\beta_\pm\left[\lambda\left(\frac{m_W^2}{m_{H^+}^2}, \frac{m_Z^2}{m_{H^+}^2}\right)\right]^{1/2}\left[2 + \frac{m_{H^+}^4}{4m_W^2 m_Z^2}\left(1 - \frac{m_W^2}{m_{H^+}^2} - \frac{m_Z^2}{m_{H^+}^2}\right)^2\right], \tag{A12}$$

$$\Gamma(H^\pm \to W^\pm Z^*) = \frac{3g^2 g_Z^4}{1024\pi^3 m_{H^+}}v_\Delta^2\cos^2\beta_\pm H\left(\frac{m_W^2}{m_{H^+}^2}, \frac{m_Z^2}{m_{H^+}^2}\right)\left(7 - \frac{40}{3}\sin^2\theta_W + \frac{160}{9}\sin^4\theta_W\right), \tag{A13}$$

$$\Gamma(H^\pm \to W^{\pm *} Z) = \frac{9g^4 g_Z^2}{512\pi^3 m_{H^+}}v_\Delta^2\cos^2\beta_\pm H\left(\frac{m_Z^2}{m_{H^+}^2}, \frac{m_W^2}{m_{H^+}^2}\right), \tag{A14}$$

$$\Gamma(H^\pm \to \hat{\varphi} W^\pm) = \frac{g^2 m_{H^+}^3}{64\pi^2 m_W^2}\xi_{H^+W^-\hat{\varphi}}^2\left[\lambda\left(\frac{m_W^2}{m_{H^+}^2}, \frac{m_{\hat{\varphi}}^2}{m_{H^+}^2}\right)\right]^{3/2}, \tag{A15}$$

$$\Gamma(H^\pm \to \hat{\varphi} W^{\pm *}) = \frac{9g^4 m_{H^+}}{512\pi^3}\xi_{H^+W^-\hat{\varphi}}^2 G\left(\frac{m_{\hat{\varphi}}^2}{m_{H^+}^2}, \frac{m_W^2}{m_{H^+}^2}\right), \tag{A16}$$

where $g_Z = g/\cos\theta_W$ with θ_W is the weak angle. The function $H(x, y)$ is

$$\begin{aligned} H(x,y) = & \frac{\arctan\left[\frac{1-x+y}{\sqrt{-\lambda(x,y)}}\right] + \arctan\left[\frac{1-x-y}{\sqrt{-\lambda(x,y)}}\right]}{4x\sqrt{-\lambda(x,y)}}\Big[-3x^3 + (9y+7)x^2 - 5(1-y)^2 x + (1-y)^3\Big] \\ & + \frac{1}{24xy}\Big\{(-1+x)[6y^2 + y(39x-9) + 2(1-x)^2] - 3y[y^2 + 2y(3x-1) - x(3x+4) + 1]\log x\Big\}. \end{aligned} \tag{A17}$$

We have confirmed that the numerical value by using Eq. (A17) coincides with that by using CalcHEP. In Eq. (A15) and Eq. (A16), $\hat{\varphi}$ denotes h, H or A and $\xi_{H^+W^-\hat{\varphi}}$ is expressed as

$$\begin{aligned}
\xi_{H^+W^-h} &= \cos\alpha\sin\beta_\pm - \sqrt{2}\sin\alpha\cos\beta_\pm, \\
\xi_{H^+W^-H} &= \sin\alpha\sin\beta_\pm + \sqrt{2}\cos\alpha\cos\beta_\pm, \\
\xi_{H^+W^-A} &= \sin\beta_0\sin\beta_\pm + \sqrt{2}\cos\beta_0\cos\beta_\pm.
\end{aligned} \tag{A18}$$

3. Decay rates of H

The decay rates for H can be evaluated as

$$\Gamma(H\to f\bar{f}) = \frac{N_c^f m_f^2 m_H}{8\pi v^2}\sin^2\alpha\left[\beta\left(\frac{m_f^2}{m_H^2}\right)\right]^3, \tag{A19}$$

$$\Gamma(H\to\nu\nu) = \Gamma(H\to\nu^c\bar{\nu}) + \Gamma(H\to\bar{\nu}^c\nu) = \sum_{i,j=1}^{3} S_{ij}|h_{ij}|^2\frac{m_H}{4\pi}\cos^2\alpha, \tag{A20}$$

$$\Gamma(H\to W^+W^-) = \frac{g^4 m_H^3}{16\pi m_W^4}\left(\frac{v}{2}\sin\alpha - v_\Delta\cos\alpha\right)^2\left(\frac{1}{4} - \frac{m_W^2}{m_H^2} + \frac{3m_W^4}{m_H^4}\right)\beta\left(\frac{m_W^2}{m_H^2}\right), \tag{A21}$$

$$\Gamma(H\to ZZ) = \frac{g_Z^4 m_H^3}{32\pi m_Z^4}\left(\frac{v}{2}\sin\alpha - 2v_\Delta\cos\alpha\right)^2\left(\frac{1}{4} - \frac{m_Z^2}{m_H^2} + \frac{3m_Z^4}{m_H^4}\right)\beta\left(\frac{m_Z^2}{m_H^2}\right), \tag{A22}$$

$$\Gamma(H\to WW^*) = \frac{3g^6 m_H}{512\pi^3}\frac{(\frac{v}{2}\sin\alpha - v_\Delta\cos\alpha)^2}{m_W^2}F\left(\frac{m_W^2}{m_H^2}\right), \tag{A23}$$

$$\Gamma(H\to ZZ^*) = \frac{g_Z^6 m_H}{2048\pi^3}\frac{(\frac{v}{2}\sin\alpha - 2v_\Delta\cos\alpha)^2}{m_Z^2}\left(7 - \frac{40}{3}\sin^2\theta_W + \frac{160}{9}\sin^4\theta_W\right)F\left(\frac{m_Z^2}{m_H^2}\right), \tag{A24}$$

$$\Gamma(H\to hh) = \frac{\lambda_{Hhh}^2}{8\pi m_H}\beta\left(\frac{m_h^2}{m_H^2}\right), \tag{A25}$$

where

$$\begin{aligned}
\lambda_{Hhh} &= \frac{1}{4v^2}\Big\{2v_\Delta\left[-2M_\Delta^2 + v^2(\lambda_4+\lambda_5)\right]\cos^3\alpha + v^3\left[-12\lambda_1 + 4(\lambda_4+\lambda_5)\right]\cos^2\alpha\sin\alpha \\
&\quad + 4v_\Delta\left[2M_\Delta^2 + v^2(3\lambda_2 + 3\lambda_3 - \lambda_4 - \lambda_5)\right]\cos\alpha\sin^2\alpha - 2v^3(\lambda_4+\lambda_5)\sin^3\alpha\Big\} \\
&\simeq \frac{1}{4v^2}\Big\{2v_\Delta\left[-2M_\Delta^2 + v^2(\lambda_4+\lambda_5)\right]\cos^3\alpha + v^3\left[-12\lambda_1 + 4(\lambda_4+\lambda_5)\right]\cos^2\alpha\sin\alpha\Big\},
\end{aligned} \tag{A26}$$

and N_c^f is the color factor with $N_c^q = 3$, $N_c^\ell = 1$.

4. Decay rates of A

The decay rates for H can be evaluated as

$$\Gamma(A\to f\bar{f}) = \sin^2\beta_0\frac{N_c^f m_f^2 m_A}{8\pi v^2}\beta\left(\frac{m_f^2}{m_A^2}\right), \tag{A27}$$

$$\Gamma(A\to\nu\nu) = \Gamma(A\to\nu^c\bar{\nu}) + \Gamma(A\to\bar{\nu}^c\nu) = \sum_{i,j=1}^{3} S_{ij}|h_{ij}|^2\frac{m_A}{4\pi}\cos^2\beta_0, \tag{A28}$$

$$\Gamma(A\to hZ) = \frac{g_Z^2 m_A^3}{64\pi m_Z^2}(\cos\alpha\sin\beta_0 - 2\sin\alpha\cos\beta_0)^2\left[\lambda\left(\frac{m_h^2}{m_A^2},\frac{m_Z^2}{m_A^2}\right)\right]^{3/2}, \tag{A29}$$

$$\Gamma(A\to hZ^*) = \frac{3g_Z^4}{1024\pi^3}(\cos\alpha\sin\beta_0 - 2\sin\alpha\cos\beta_0)^2 m_A G\left(\frac{m_h^2}{m_A^2},\frac{m_Z^2}{m_A^2}\right)\left(7 - \frac{40}{3}\sin^2\theta_W + \frac{160}{9}\sin^4\theta_W\right). \tag{A30}$$

[1] Update of the combination of Higgs boson searches in 1.0 to 2.3 fb^{-1} of pp collisions data taken at $\sqrt{s} = 7$ TeV with the ATLAS experiment at the LHC, ATLAS-CONF-2011-135; Search for standard model Higgs boson in pp collisions at $\sqrt{s} = 7$ TeV and integrated luminosity up to 1.7 fb^{-1}, CMS PAS HIG-11-022.

[2] T. Schwetz, M. A. Tortola, J. W. F. Valle, New J. Phys. **10**, 113011 (2008).

[3] E. Komatsu *et al.* [WMAP Collaboration], Astrophys. J. Suppl. **192**, 18 (2011).

[4] A. D. Sakharov, Pisma Zh. Eksp. Teor. Fiz. **5**, 32-35 (1967).

[5] P. Minkowski, Phys. Lett. B **67**, 421 (1977); T. Yanagida, In Proceedings of Workshop on *the Unified Theory and the Baryon Number in the Universe*, p.95 KEK Tsukuba, Japan (1979); M. Gell-Mann, P. Ramond and R. Slansky, in Proceedings of Workshop *Supergravity*, p.315, Stony Brook, New York, 1979. R. N. Mohapatra and G. Senjanovic, Phys. Rev. Lett. **44**, 912 (1980).

[6] T. P. Cheng and L. F. Li, Phys. Rev. D **22**, 2860 (1980); J. Schechter and J. W. F. Valle, Phys. Rev. D **22**, 2227 (1980); G. Lazarides, Q. Shafi and C. Wetterich, Nucl. Phys. B **181**, 287 (1981); R. N. Mohapatra and G. Senjanovic, Phys. Rev. D **23**, 165 (1981); M. Magg and C. Wetterich, Phys. Lett. B **94**, 61 (1980).

[7] R. Foot, H. Lew, X. G. He and G. C. Joshi, Z. Phys. C **44**, 441 (1989).

[8] J. F. Gunion, C. Loomis and K. T. Pitts, *In the Proceedings of 1996 DPF / DPB Summer Study on New Directions for High-Energy Physics (Snowmass 96), Snowmass, Colorado, 25 Jun - 12 Jul 1996, pp LTH096* [arXiv:hep-ph/9610237].

[9] M. Muhlleitner and M. Spira, Phys. Rev. D **68**, 117701 (2003); T. Han, B. Mukhopadhyaya, Z. Si and K. Wang, Phys. Rev. D **76**, 075013 (2007); A. G. Akeroyd, C. W. Chiang and N. Gaur, JHEP **1011**, 005 (2010).

[10] E. J. Chun, K. Y. Lee and S. C. Park, Phys. Lett. B **566**, 142 (2003); A. G. Akeroyd and M. Aoki, Phys. Rev. D **72**, 035011 (2005).

[11] P. Fileviez Perez, T. Han, G. -y. Huang, T. Li, K. Wang, Phys. Rev. **D78**, 015018 (2008).

[12] A. G. Akeroyd, H. Sugiyama, Phys. Rev. **D84**, 035010 (2011).

[13] A. Melfo, M. Nemevsek, F. Nesti, G. Senjanovic and Y. Zhang, arXiv:1108.4416 [hep-ph].

[14] J. Garayoa and T. Schwetz, JHEP **0803**, 009 (2008); A. G. Akeroyd, M. Aoki and H. Sugiyama, Phys. Rev. D **77**, 075010 (2008); F. del Aguila and J. A. Aguilar Saavedra, Nucl. Phys. B **813**, 22 (2009); A. G. Akeroyd and C. W. Chiang, Phys. Rev. D **80**, 113010 (2009).

[15] M. Kadastik, M. Raidal and L. Rebane, Phys. Rev. D **77**, 115023 (2008).

[16] Talk by A. K. Nayak (CMS Collaboration) at Europhysics Conference on High-Energy Physics 2011, July 22 2011, Grenoble, France; talk by H. Bachacou at the Symposium on Lepton-Photon Interactions, Mumbai, India, August 22-27 2011.

[17] S. Chakrabarti, D. Choudhury, R. M. Godbole and B. Mukhopadhyaya, Phys. Lett. B **434**, 347 (1998).

[18] A. Zee, Nucl. Phys. B **264**, 99 (1986); K. S. Babu, Phys. Lett. B **203**, 132 (1988); M. Aoki, S. Kanemura, T. Shindou, K. Yagyu, JHEP **1007**, 084 (2010).

[19] M. Aoki, S. Kanemura, K. Yagyu, Phys. Lett. **B702**, 355-358 (2011).

[20] V. Rentala, W. Shepherd, S. Su, Phys. Rev. **D84**, 035004 (2011).

[21] P. Dey, A. Kundu and B. Mukhopadhyaya, J. Phys. G **36**, 025002 (2009); A. Arhrib, R. Benbrik, M. Chabab, G. Moultaka, M. C. Peyranere, L. Rahili, J. Ramadan, [arXiv:1105.1925 [hep-ph]].

[22] K. Nakamura *et al.* [Particle Data Group], J. Phys. G **37**, 075021 (2010).

[23] T. Blank and W. Hollik, Nucl. Phys. B **514**, 113 (1998).

[24] M. Czakon, J. Gluza, F. Jegerlehner and M. Zralek, Eur. Phys. J. C **13**, 275 (2000).

[25] J. R. Forshaw, D. A. Ross and B. E. White, JHEP **0110**, 007 (2001).

[26] J. R. Forshaw, A. Sabio Vera and B. E. White, JHEP **0306**, 059 (2003).

[27] M. C. Chen, S. Dawson and T. Krupovnickas, Phys. Rev. D **74**, 035001 (2006).

[28] P. H. Chankowski, S. Pokorski and J. Wagner, Eur. Phys. J. C **50**, 919 (2007).

[29] M. C. Chen, S. Dawson and C. B. Jackson, Phys. Rev. D **78**, 093001 (2008).

[30] E. Asakawa, S. Kanemura, Phys. Lett. **B626**, 111-119 (2005); E. Asakawa, S. Kanemura, J. Kanzaki, Phys. Rev. **D75**, 075022 (2007).

[31] K. -m. Cheung, R. J. N. Phillips, A. Pilaftsis, Phys. Rev. **D51**, 4731-4737 (1995); S. Kanemura, K. Yagyu, K. Yanase, Phys. Rev. **D83**, 075018 (2011).

[32] A. Pukhov, [hep-ph/0412191].

[33] M. Ciuchini, G. Degrassi, P. Gambino and G. F. Giudice, Nucl. Phys. B **527**, 21 (1998).

[34] Q. -H. Cao, S. Kanemura, C. P. Yuan, Phys. Rev. **D69**, 075008 (2004); Q. -H. Cao, D. Nomura, K. Tobe, C. -P. Yuan, Phys. Lett. **B632**, 688-694 (2006); A. Belyaev, Q. -H. Cao, D. Nomura, K. Tobe, C. -P. Yuan, Phys. Rev. Lett. **100**, 061801 (2008).

[35] M. Aoki, S. Kanemura, K. Tsumura and K. Yagyu, Phys. Rev. D **80** (2009) 015017.

[36] A. Djouadi, J. Kalinowski, P. M. Zerwas, Z. Phys. **C70**, 435-448 (1996).